

Adversarial Radar Inference: Inverse Tracking, Identifying Cognition and Designing Smart Interference

Vikram Krishnamurthy, *Fellow, IEEE*, Kunal Pattanayak, *Student Member, IEEE*, Sandeep Gogineni, *Member, IEEE*, Bosung Kang, *Member, IEEE*, Muralidhar Rangaswamy, *Fellow, IEEE*

Abstract—This paper considers three inter-related adversarial inference problems involving cognitive radars. We first discuss inverse tracking of the radar to estimate the adversary’s estimate of us based on the radar’s actions and calibrate the radar’s sensing accuracy. Second, using revealed preference from microeconomics, we formulate a non-parametric test to identify if the cognitive radar is a constrained utility maximizer with signal processing constraints. We consider two radar functionalities, namely, beam allocation and waveform design, with respect to which the cognitive radar is assumed to maximize its utility and construct a set-valued estimator for the radar’s utility function. Finally, we discuss how to engineer interference at the physical layer level to confuse the radar which forces it to change its transmit waveform. The levels of abstraction range from smart interference design based on Wiener filters (at the pulse/waveform level), inverse Kalman filters at the tracking level and revealed preferences for identifying utility maximization at the systems level.

Index Terms—Inverse Tracking, Smart Interference, Revealed Preference, Constrained Utility Maximization, Kalman filter, Bayesian Inference, Physical Layer Interference, Adversarial Inference, Radar Signal Processing

This research was supported in part by the US Army Research Office under grants W911NF-21-1-0093 and W911NF-19-1-0365, and the National Science Foundation under grant CCF-1714180.

V. Krishnamurthy and K. Pattanayak are with the School of Electrical and Computer Engineering, Cornell University, Ithaca, NY, 14853 USA. e-mail: vikramk@cornell.edu, kp87@cornell.edu.

S. Gogineni is with the Information Systems Laboratories, Inc., San Diego, CA, USA. e-mail: sgogineni@islinc.com.

B. Kang is with the University of Dayton Research Institute, Dayton, OH, 45469 USA. e-mail: Bosung.Kang@udri.udayton.edu.

M. Rangaswamy is with the Air Force Research Laboratory, Wright Patterson Air Force Base, OH, 45433 USA. e-mail: Muralidhar.Rangaswamy@us.af.mil.

Glossary of Symbols.

Inverse Tracking (Sec. II)

x_k	our kinematic state at time k
P_{x_{k+1}, x_k}	transition kernel $p(x_{k+1} x_k)$
w_k	state noise at time k
Q_k	covariance of w_k
y_k	observation of x_k
v_k	observation noise at time k
R_k	covariance of v_k
C	adversary sensor gain
B_{x_k, y_k}	conditional pdf of y_k given state x_k $p(y_k x_k)$
π_k	adversary’s belief of x_k
$T(\pi, y)$	belief update
\hat{x}_k	conditional mean of state estimate of x_k
Σ_k	covariance of state estimate of x_k
u_k	adversary’s action at time k
ϕ	stochastic mapping from π_k to u_k
a_k	our measurement of u_k
G_{π_k, a_k}	conditional pdf of a_k given belief π_k $p(a_k \pi_k)$
ρ_k	our belief of π_k given x_k and a_k
$\hat{\hat{x}}_k$	conditional mean of \hat{x}_k
$\bar{\Sigma}_k$	covariance of $\hat{\hat{x}}_k$
θ	model parameter for C
L_N	log-likelihood
ι_k	innovations of inverse Kalman filter

Identifying Cognition (Sec. III)

n	slow time scale index
α_n	probe signal at time n
β_n	adversary’s response at time n
$U(\beta)$	adversary’s utility function

Smart Interference (Sec. IV)

\mathbf{X}_l	adversary radar’s received signal at l^{th} pulse
$\mathbf{H}_t(l)$	transmit channel impulse response at l^{th} pulse
$\mathbf{H}_c(l)$	clutter channel impulse response at l^{th} pulse
$\mathbf{H}_p(l)$	probe signal at l^{th} pulse
$\mathbf{W}(l)$	radar’s transmission waveform at l^{th} pulse
$\mathbf{E}_r(l)$	measurement noise in $\mathbf{X}(l)$
C_r	covariance of $\mathbf{E}_r(l)$
$\mathbf{Y}(l)$	our observation of $\mathbf{W}(l)$
$\mathbf{E}_o(l)$	measurement noise in $\mathbf{Y}(l)$
C_o	covariance of $\mathbf{E}_o(l)$

I. INTRODUCTION

Cognitive sensors are reconfigurable sensors that optimize their sensing mechanism and transmit functionalities. The con-

cept of cognitive radar [11], [26], [27], [20] has evolved over the last two decades and a common aspect is the sense-learn-adapt paradigm. A cognitive fully adaptive radar enables joint optimization of the adaptive transmit and receive functions by sensing (estimating) the radar channel that includes clutter and other interfering signals [5], [18].

A. Objectives

This paper addresses the next step and achieves the following objectives schematically shown in Figure 1. The framework in this paper involves an adversarial signal processing problem comprising “us” and an “adversary”. “Us” refers to an asset such as a drone/UAV or electromagnetic signal that probes an “adversary” cognitive radar. Figure 2 shows the schematic setup. A cognitive sensor observes our kinematic state x_k in noise as the observation y_k . It then uses a Bayesian tracker to update its posterior distribution π_k of our state x_k and chooses an action u_k based on this posterior. We observe the sensor’s action in noise as a_k . Given knowledge of “our” state sequence $\{x_k\}$ and the observed actions $\{a_k\}$ taken by the adversary’s sensor, we focus on the following inter-related aspects:

1. Inverse tracking and estimating the Adversary’s Sensor Gain. Suppose the adversary radar observes our state in noise; updates its posterior distribution π_k of our state x_k using a Bayesian tracker, and then chooses an action u_k based on this posterior. Given knowledge of “our” state and sequence of noisy measurements $\{a_k\}$ of the adversary’s actions $\{u_k\}$, how can the adversary radar’s posterior distribution (random measure) be estimated? We will develop an inverse Bayesian filter for tracking the radar’s posterior belief of our state and present an example involving the Kalman filter where the inverse filtering problem admits a finite dimensional characterization.

A related question is: How to remotely estimate the adversary radar sensor’s conditional pdf of observation given the state when it is estimating us? This is important because it tells us how accurate the adversary’s sensor is; in the context of Figure 2 it tells us, how accurately the adversary tracks our drone. The data we have access to is our state (probe signal) sequence $\{x_k\}$ and measurements of the adversary’s radar actions $\{a_k\}$. Estimating the adversary’s sensor accuracy is non-trivial with several challenges. First, even though we know our state and state dynamics model (transition law), the adversary does not. The adversary needs to estimate our state and state transition law based on our trajectory; and we need to estimate the adversary’s estimate of our state transition law. Second, computing the MLE of the adversary’s sensor gain also requires inverse filtering.

2. Revealed Preferences and Identifying Cognitive Radars. Suppose the cognitive radar is a constrained utility maximizer that optimizes its actions u_k subject to physical level (Bayesian filter) constraints. How can we detect this utility maximization behavior? The actions u_k can be viewed as resources the radar adaptively allocates to maximize its utility. We consider two such resource allocation problems, namely,

- *Beam Allocation:* The radar adaptively switches its beam while tracking multiple targets.
- *Waveform Design:* The radar adaptively designs its waveform while ensuring the signal-to-interference-plus-noise ratio (SINR) exceeds a pre-defined threshold.

Nonparametric detection of utility maximization behavior is the central theme of *revealed preference* in microeconomics. A remarkable result is *Afriat’s theorem*: it provides a necessary and sufficient condition for a finite dataset to have originated from a utility maximizer. We will develop constrained set-valued utility estimation methods that account for signal processing constraints introduced by the Bayesian tracker for performing adaptive beam allocation and waveform design respectively.

3. Smart Signal Dependent Interference. We next consider the adversary radar choosing its transmit waveform for target tracking by implementing a Wiener filter to maximize its signal-to-clutter-plus-noise ratio (SCNR¹). By observing the optimal waveform chosen by the radar, our aim is to develop a strategy to estimate the adversary cognitive radar channels and then construct signal dependent interference generation to confuse the adversary radar.

B. Perspective

The adversarial dynamics considered in this paper fit naturally within the so called Dynamic Data and Information Processing (DDIP) paradigm. The adversary’s radar senses, adapts and learns from us. In turn we adapt, sense and learn from the adversary. So in simple terms we are modeling and analyzing the interaction of two DDIP systems. In this context, this paper has three major themes schematically shown in Figure 1: inverse filtering which is a Bayesian framework for interacting DDIP systems, inverse cognitive sensing which is a non-parametric approach for utility estimation for interacting DDIP systems, and interference design to confuse the adversarial DDIP system.

This work is also motivated by the design of counter-autonomous systems: given measurements of the actions of an autonomous adversary, how can our counter-autonomous system estimate the underlying belief of the adversary, identify if the adversary is cognitive (constrained utility maximizer) and design appropriate probing signals to confuse the adversary. This paper generalizes and contextualizes recent works in adversarial signal processing [29], [25] which only deal with specific radar functionalities. Instead, this paper views the cognitive radar as a holistic system operating at three stages of sophistication unifies the three inter-related aspects of adversarial signal processing, namely, inverse tracking, identifying cognition and designing interference. The three components complement one another and constitute this paper’s adversarial signal processing sense-learn-adapt (SLA) paradigm of Figure 1.

C. Organization

We conclude this section with a brief outline of the key results of the following sections, and their relevant to the sense,

¹The terms SCNR and SINR are used interchangeably in the paper.

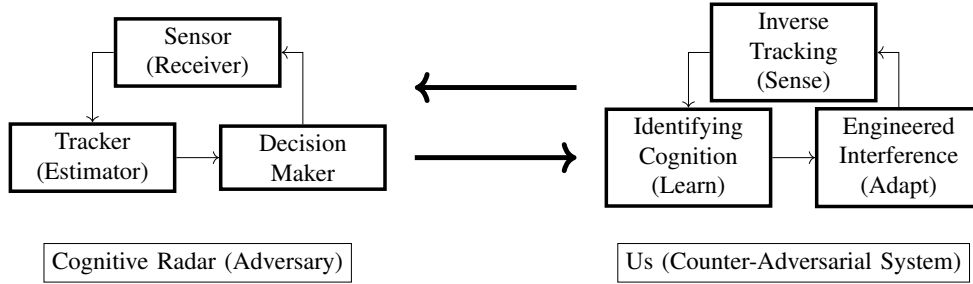


Fig. 1: Schematic illustrating the main ideas in the paper. The three components on the right are inter-related and constitute the sense-learn-adapt paradigm of the observer (“us”) reacting to a reactive system such as the cognitive radar (on the left). This paper considers the above schematic and proposes counter-adversarial schemes against cognitive radars for different levels of abstraction, i.e., interference design based on Wiener filters at the pulse/waveform level, inverse Kalman filters at the Bayesian tracking level, and revealed preference techniques for estimating adversary’s utility function at the systems level.

learn and adapt elements of the SLA paradigm of Figure 1.

Sense: In Sec. II, we discuss inverse tracking techniques to estimate the sensor accuracy of an adversary radar. We focus mainly on the inverse Kalman filter and illustrate in carefully chosen examples how the adversary sensor’s accuracy can be estimated. This constitutes the ‘sensing’ aspect of the SLA paradigm.

Learn: In Sec. III, we abstractly view the adversarial radar as a cognitive decision maker that maximizes a utility function subject to physical resource constraints. Specifically, we show that if the cognitive radar optimizes its waveform to maintain its SINR above a threshold, then we can identify (and hence, ‘learn’) the utility function of the radar. The utility function provides deeper knowledge of the radar’s behavior and constitutes the ‘learn’ element of the SLA paradigm.

Adapt: In Sec. IV, we consider a slightly modified setup where the radar chooses its waveform to maximize its SCNR. We show that by intelligently probing the radar with interference signals and observing the changes in the radar’s waveform, we can confuse the adversary’s radar by decreasing its SCNR. This adaptive signal processing algorithm is justified only if the ‘sense’ and ‘learn’ aspect of the SLA paradigm function properly, that is, the counter-adversarial system knows how the radar will react to changes in its environment.

Finally, we emphasize that the three main aspects of inverse tracking (sensing the estimate of the adversary), identifying utility maximization (learning the adversary’s utility function) and adaptive interference (adapting our response) are instances of the general paradigm of sense-learn-adapt in counter-adversarial systems. As mentioned above, our formulation deals with the interaction of two such sense-learn-adapt systems.

II. INVERSE TRACKING AND ESTIMATING ADVERSARY’S SENSOR

This section discusses inverse tracking in an adversarial system schematically illustrated in Figure 2. Our main ideas involve estimating the adversary’s estimate of us and estimating the adversary’s sensor conditional pdf of observation given the state.

A. Background and Preliminary Work

We start by formulating the problem which involves two entities; “us” and “adversary”. With $k = 1, 2, \dots$ denoting discrete time, the model has the following dynamics:

$$\begin{aligned} x_k &\sim P_{x_{k-1}, x} = p(x|x_{k-1}), & x_0 &\sim \pi_0 \\ y_k &\sim B_{x_k, y} = p(y|x_k) \\ \pi_k &= T(\pi_{k-1}, y_k) = p(x_k|y_{1:k}) \\ a_k &\sim G_{\pi_k, a} = p(a|\pi_k) \end{aligned} \quad (1)$$

Let us explain the notation in (1):

- $x_k \in \mathcal{X}$ is our Markovian state with transition kernel $P_{x_{k-1}, x}$, prior π_0 and state space \mathcal{X} .
- y_k is the adversary’s noisy observation of our state x_k ; with conditional pdf of observation given the state $B_{x_k, y}$.
- π_k is the adversary’s belief (posterior) of our state x_k where $y_{1:k}$ denotes the observation sequence y_1, \dots, y_k . The operator T in (1) is the classical Bayesian optimal filter that computes the posterior belief of the state given observation y and current belief π .

$$T(\pi, y) = \text{vec} \left(\frac{B_{x, y} \int_{\mathcal{X}} P_{\zeta, x} \pi(\zeta) d\zeta}{\int_{\mathcal{X}} B_{x, y} \int_{\mathcal{X}} P_{\zeta, x} \pi(\zeta) d\zeta dx}, x \in \mathcal{X} \right) \quad (2)$$

Let Π denote the space of all such beliefs. When the state space \mathcal{X} is finite, then Π is the unit $X - 1$ dimensional simplex of X -dimensional probability mass functions.

- a_k denotes our measurement of the adversary’s action based on its current belief π_k . The adversary chooses an action u_k as a (possibly) stochastic function of π_k and we obtain a noisy measurement of u_k as a_k . We encode this as G_{π_k, a_k} , the conditional probability of observing action a_k given the adversary’s belief π_k . Although not explicitly shown, G abstracts two stochastic maps: 1) the map from the adversary’s belief π_k to its action u_k , and 2) the map from the adversary’s action u_k to our noisy measurement a_k of this action.

Figure 2 displays a schematic and graphical representation of the model (1). The schematic model shows “us” and the adversary’s variables.

Aim: Referring to model (1) and Figure 2, we address the following questions in this section:

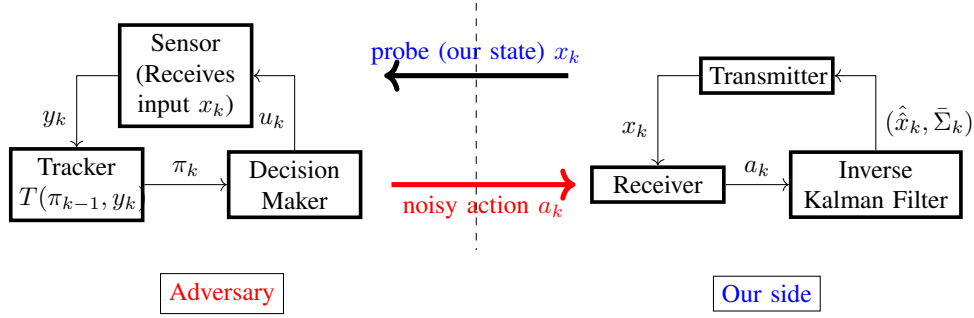


Fig. 2: Schematic of Adversarial Inference Problem. Our side is a drone/UAV or electromagnetic signal that probes the adversary’s cognitive radar system. Based on the action a_k of the adversary, our side computes the estimate of the adversary’s estimate of our state x_k using the inverse Kalman filter outlined in Sec. II-B.

- 1) How to estimate the adversary’s belief given measurements of its actions (which are based on its filtered estimate of our state)? In other words, assuming probability distributions P, B, G are known², we aim to estimate the adversary’s belief π_k at each time k , by computing posterior $p(\pi_k | \pi_0, x_{0:k}, a_{1:k})$.
- 2) How to estimate the adversary’s observation kernel B , i.e. its sensor gain? This tells us how accurate the adversary’s sensor is.

From a practical point of view, estimating the adversary’s belief and sensor parameters allows us to calibrate its accuracy and predict (in a Bayesian sense) future actions of the adversary.

Related Works. In recent works [34], [35], [33], the mapping from belief π to adversary’s action u was assumed deterministic. In comparison, our proposed research here assumes a probabilistic map between π and a and we develop Bayesian filtering algorithms for estimating the posterior along with MLE (Maximum Likelihood Estimation) algorithms for estimating the underlying model. Estimating/reconstructing the posterior given decisions based on the posterior is studied in microeconomics under the area of social learning [10] and game-theoretic generalizations [4]. There are strong parallels between inverse filtering and Bayesian social learning [10], [24], [23], [22]; the key difference is that social learning aims to estimate the underlying state given noisy posteriors, whereas our aim is to estimate the posterior given noisy measurements of the posterior and the underlying state. Recently, [21] used cascaded Kalman filters for LQG control over communication channels. This work motivates the design of the function ϕ in (8) below that maps the adversary’s belief to its action; see also footnote 5. Finally, in [12], the authors investigate the inverse problem of trajectory identification based on target measurements, where the target is assumed to follow a constant velocity model.

B. Inverse Tracking Algorithms

How to estimate the adversary’s posterior distribution of us?

²As mentioned in footnote 6, this assumption simplifies the setup; otherwise we need to estimate the adversary’s estimate of us, which makes our task substantially complex.

Here we discuss inverse tracking for the model (1). Define the posterior distribution $\rho_k(\pi_k) = p(\pi_k | a_{1:k}, x_{0:k})$ of the adversary’s posterior distribution given our state sequence $x_{0:k}$ and actions $a_{1:k}$. Note that the posterior $\rho_k(\cdot)$ is a *random measure* since it is a posterior distribution of the adversary’s posterior distribution (belief) π_k . By using a discrete time version of Girsanov’s theorem and appropriate change of measure³ [15] (or a careful application of Bayes rule) we can derive the following functional recursion for ρ_k (see [29])

$$\rho_{k+1}(\pi) = \frac{G_{\pi, a_{k+1}} \int_{\Pi} B_{x_{k+1}, y_{\pi_k, \pi}} \rho_k(\pi_k) d\pi_k}{\int_{\Pi} G_{\pi, a_{k+1}} \int_{\Pi} B_{x_{k+1}, y_{\pi_k, \pi}} \rho_k(\pi_k) d\pi_k d\pi} \quad (3)$$

Here $y_{\pi_k, \pi}$ is the observation such that $\pi = T(\pi_k, y)$ where T is the adversary’s filter (2). We call (3) the *optimal inverse filter* since it yields the Bayesian posterior of the adversary’s belief given our state and noisy measurements of the adversary’s actions.

Example: Inverse Kalman Filter

We consider a special case of (3) where the inverse filtering problem admits a finite dimensional characterization in terms of the Kalman filter. Consider a linear Gaussian state space model

$$\begin{aligned} x_{k+1} &= A x_k + w_k, & x_0 &\sim \pi_0 \\ y_k &= C x_k + v_k \end{aligned} \quad (4)$$

where $x_k \in \mathcal{X} = \mathbb{R}^X$ is “our” state with initial density $\pi_0 \sim \mathbf{N}(\hat{x}_0, \Sigma_0)$, $y_k \in \mathcal{Y} = \mathbb{R}^Y$ denotes the adversary’s observations, $w_k \sim \mathbf{N}(0, Q_k)$, $v_k \sim \mathbf{N}(0, R_k)$ and $\{w_k\}$, $\{v_k\}$ are mutually independent i.i.d. processes. Here, $\mathbf{N}(\mu, C)$ denotes the normal distribution with mean μ and covariance matrix C .

Based on observations $y_{1:k}$, the adversary computes the belief $\pi_k = \mathbf{N}(\hat{x}_k, \Sigma_k)$ where \hat{x}_k is the conditional mean state

³This paper deals with discrete time. Although we will not pursue it here, the recent paper [28] uses a similar continuous time formulation. This yields interesting results involving Malliavin derivatives and stochastic calculus.

The likelihood can be evaluated from the un-normalized inverse filtering recursion (3)

$$L_N(\theta) = \log \int_{\Pi} q_N^\theta(\pi) d\pi, \\ q_{k+1}^\theta(\pi) = G_{\pi, a_{k+1}} \int_{\Pi} B_{x_{k+1}, y_{\pi_k, \pi}}^\theta q_k^\theta(\pi_k) d\pi_k, \quad (14)$$

initialized by setting $q_0^\theta(\pi_0) = \pi_0$. Here $y_{\pi_k, \pi}$ is the observation such that $\pi = T(\pi_k, y)$ where T is the adversary's filter (2) with variable B parametrized by θ . Given (14), a local stationary point of the likelihood can be computed using a general purpose numerical optimization algorithm.

D. Example. Estimating Adversary's Gain in Linear Gaussian case

The aim of this section is to provide insight into the nature of estimating the adversary's sensor gain via numerical examples. Consider the setup in Sec.II-B where our dynamics are linear Gaussian and the adversary observes our state linearly in Gaussian noise (4). The adversary estimates our state using a Kalman filter, and we estimate the adversary's estimate using the inverse Kalman filter (9). Using (9), (10), the log-likelihood for the adversary's observation gain matrix $\theta = C$ based on our measurements is⁷

$$L_N(\theta) = \text{const} - \frac{1}{2} \sum_{k=1}^N \log |\bar{S}_k^\theta| - \frac{1}{2} \sum_{k=1}^N \iota_k' (\bar{S}_k^\theta)^{-1} \iota_k \\ \iota_k = a_k - \bar{C}_k^\theta \bar{A}_{k-1}^\theta \hat{x}_{k-1} - \bar{F}_{k-1}^\theta x_{k-1} \quad (15)$$

where ι_k are the innovations of the inverse Kalman filter (11). In (15), our state x_{k-1} is known to us and therefore is a known exogenous input. Also note from (10) that \bar{A}_k, \bar{F}_k are explicit functions of C , while \bar{C}_k and \bar{Q}_k depend on C via the adversary's Kalman filter.

The log-likelihood for the adversary's observation gain matrix $\theta = C$ can be evaluated using (15). To provide insight, Figure 3 displays the log-likelihood versus adversary's gain matrix C in the scalar case for 1000 equally spaced data points over the interval $C = (0, 10]$. The four sub-figures correspond to true values $C^o = 2.5, 3.5$ of C , respectively.

Each sub-figure in Figure 3 has two plots. The plot in red is the log-likelihood of $\hat{C} \in (0, 10]$ evaluated based on the adversary's observations using the standard Kalman filter. (This is the classical log-likelihood of the observation gain of a Gaussian state space model.) The plot in blue is the log-likelihood of $C \in (0, 10]$ computed using our measurements of the adversary's action using the inverse Kalman filter (where the adversary first estimates our state using a Kalman filter) - we call this the inverse case.

Figure 3 shows that the log-likelihood in the inverse case (blue plots) has a less pronounced maximum compared to the standard case (red plots). Therefore, numerical algorithms for computing the MLE of the adversary's gain C^o using our observations of the adversary's actions (via the inverse Kalman filter) will converge much more slowly than the classical MLE (based on the adversary's observations). This is intuitive since

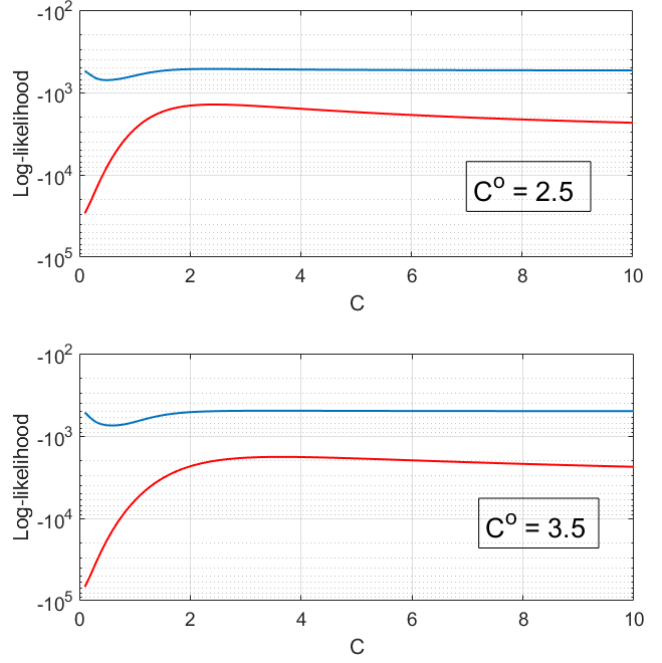


Fig. 3: Log-Likelihood as a function of adversary's gain $C \in (0, 10]$ when true value is C^o . The red curves denote the log-likelihood of C given the adversary's measurements of our state. The blue curves denote the log-likelihood of C using the inverse Kalman filter given our observations of the adversary's action u_k . The plots show that it is more difficult to compute the MLE (13) for the inverse filtering problem due to the almost flat likelihood (blue curves) compared to red curves.

our estimate of the adversary's parameter is based on the adversary's estimate of our state and so has more noise.

Sensitivity of MLE. It is important to evaluate the sensitivity of the MLE of C wrt covariance matrices Q_k, R_k in the state space model (4). For example, the sensitivity wrt Q_k reveals how sensitive the MLE is wrt our maneuver covariance since from (4), Q_k determines our maneuvers. Our sensitivity analysis evaluates the variation of the second derivative of the log-likelihood of C computed at the true gain C^o to small changes in Q_k and R_k . Table I displays our sensitivity results wrt the scalar setup of Figure 3. Table I comprises two sensitivity values,

$$\eta_Q = \frac{\partial}{\partial Q_k} \left(\frac{\partial^2 L_N(\theta)}{\partial \theta^2} \right) \Bigg|_{\theta=C^o} \quad \text{and} \\ \eta_R = \frac{\partial}{\partial R_k} \left(\frac{\partial^2 L_N(\theta)}{\partial \theta^2} \right) \Bigg|_{\theta=C^o}, \quad (16)$$

evaluated for both the inverse case (that uses the inverse Kalman filter (15)) and the classic case where the adversary's observations are known. $\eta_{(\cdot)}$ measures the change in the sharpness of the log-likelihood plot around the true sensor gain wrt change in the noise covariance. Note that the experimental setup of Figure 3 assumes the covariances Q_k, R_k are constant over time index k , hence we drop the subscript in the LHS of (16).

⁷The variable θ is introduced only for notational clarity.

	C°	Classic	Inverse
η_Q	2.5	-43.45	-6.46
	3.5	-25.16	-2.77
η_R	2.5	-189.39	-50.04
	3.5	-65.27	-30.55

TABLE I: Comparison of sensitivity values (16) for log-likelihood of C wrt noise covariances Q_k , R_k (4) - classical model vs inverse Kalman filter model.

C°	Classic	Inverse
0.5	0.24×10^{-3}	5.3×10^{-3}
1.5	1.2×10^{-3}	37×10^{-3}
2	2.1×10^{-3}	70×10^{-3}
3	4.6×10^{-3}	336×10^{-3}

TABLE II: Comparison of Cramér-Rao bounds for C - classical model vs inverse Kalman filter model.

Table I shows that the second derivative of the log-likelihood is more sensitive (in magnitude) to the adversary's observation covariance R_k than the maneuver covariance Q_k . Also, it is observed that the sensitivity of the log-likelihood is higher for lower sensor gain C° . This observation is consistent with intuition since a larger gain C implies a larger SNR (signal-to-noise ratio) of the observation y_k which intuitively suggests the estimate of C is more robust to changes in maneuver covariance and observation noise covariance.

Cramér-Rao (CR) bounds. It is instructive to compare the CR bounds for MLE of C for the classic model versus that of the inverse Kalman filter model. Table II displays the CR bounds (reciprocal of expected Fisher information) for the four examples considered above evaluated using via the algorithm in [9]. It shows that the covariance lower bound for the inverse case is substantially higher than that for the classic case. This is consistent with the intuition that estimating the adversary's parameter based on its actions (which is based on its estimate of us) is more difficult than directly estimating C in a classical state space model based on the adversary's observations of our state that determines its actions.

Consistency of MLE. The above example (Figure 3) shows that the likelihood surface of $L_N(\theta) = \log p(x_{0:N}, a_{1:N} | \theta)$ is flat and hence computing the MLE numerically can be difficult. Even in the case when we observe the adversary's actions perfectly, [34] shows that non-trivial observability conditions need to be imposed on the system parameters.

For the linear Gaussian case where we observe the adversary's Kalman filter in noise, strong consistency of the MLE for the adversary's gain matrix C can be established fairly straightforwardly. Specifically, if we assume that state matrix A is stable, and the state space model is an identifiable minimal realization, then the adversary's Kalman filter variables converge to steady state values geometrically fast in k [3] implying that asymptotically the inverse Kalman filter system is stable linear time invariant. Then, the MLE θ^* for the adversary's observation matrix C is unique and strongly consistent [6].

III. IDENTIFYING UTILITY MAXIMIZATION IN A COGNITIVE RADAR

The previous section was concerned with estimating the adversary's posterior belief and sensor accuracy. This section discusses detecting utility maximization behavior and estimating the adversary's utility function in the context of cognitive radars. As described in the introduction, inverse tracking, identifying utility maximization and designing interference to confuse the radar constitute our adversarial setting.

Cognitive radars [19] use the perception-action cycle of cognition to sense the environment and learn from it relevant information about the target and the environment. The cognitive radars then tune the radar sensor to optimally satisfy their mission objectives. Based on its tracked estimates, the cognitive radar adaptively optimizes its waveform, aperture, dwell time and revisit rate. In other words, a cognitive radar is a constrained utility maximizer.

This section is motivated by the next logical step, namely, *identifying a cognitive radar* from the actions of the radar. The adversary cognitive radar observes our state in noise; it uses a Bayesian estimator (target tracking algorithm) to update its posterior distribution of our state and then chooses an action based on this posterior. From the intercepted emissions of an adversary's radar, we address the following question: Are the adversary sensor's actions consistent with optimizing a monotone utility function (i.e., is the cognitive sensor behavior rational in an economics sense)? If so how can we estimate a utility function of the adversary's cognitive sensor that is consistent with its actions? The main synthesis/analysis framework we will use is that of revealed preferences [40], [16], [14] from microeconomics which aims to determine preferences by observing choices. The results presented below are developed in detail in the recent work [25]; however, the SINR constraint formulation in Sec. III-C for detecting waveform optimization is new. Related work that develops adversarial inference strategies at a higher level of abstraction than tracking level (like the Bayesian filter level in Sec. II) includes [30]. [30] places counter unmanned autonomous systems at a level of abstraction above the physical sensors/actuators/weapons and datalink layers; and below the human controller layer.

A. Background. Revealed Preferences and Afriat's Theorem

Non-parametric detection of utility maximization behavior is studied in the area of revealed preferences in microeconomics. A key result is the following:

Definition III.1 ([1], [2]). *A system is a utility maximizer if for every probe $\alpha_n \in \mathbb{R}_+^m$, the response $\beta_n \in \mathbb{R}^m$ satisfies*

$$\beta_n \in \operatorname{argmax}_{\alpha'_n \beta \leq 1} U(\beta) \quad (17)$$

where $U(\beta)$ is a monotone utility function.

In economics, α_n is the price vector and β_n the consumption vector. Then $\alpha'_n \beta \leq 1$ is a natural budget constraint⁸ for

⁸The budget constraint $\alpha'_n \beta \leq 1$ is without loss of generality, and can be replaced by $\alpha'_n \beta \leq c$ for any positive constant c . A more general nonlinear budget incorporating spectral constraints will be discussed below.

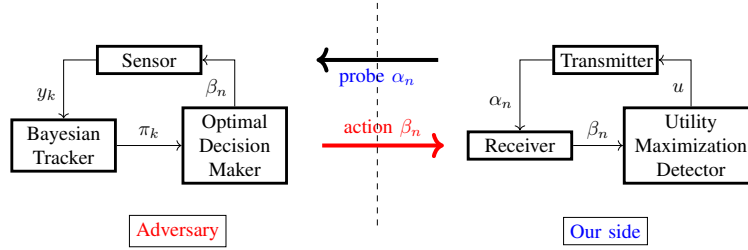


Fig. 4: Schematic of Adversarial Inference Problem. Our side is a drone/UAV or electromagnetic signal that probes the adversary’s cognitive radar system. k denotes a fast time scale and n denotes a slow time scale. Our state x_k , parameterized by α_n (purposeful acceleration maneuvers), probes the adversary radar. Based on the noisy observation y_k of our state, the adversary radar responds with action β_n . Our aim (in the Utility Maximization Detector block) is to detect if the adversary radar is economic rational, i.e., is its response β_n generated by constrained optimizing a utility function u , and if so, estimate the utility function.

a consumer with 1 dollar. Given a dataset of price and consumption vectors, the aim is to determine if the consumer is a utility maximizer (rational) in the sense of (17).

The key result is the following theorem due to Afriat [14], [2], [1], [40], [38]

Theorem III.2 (Afriat’s Theorem [1]). *Given a data set $\mathcal{D} = \{(\alpha_n, \beta_n), n \in \{1, 2, \dots, N\}\}$, the following statements are equivalent:*

- 1) *The system is a utility maximizer and there exists a monotonically increasing, continuous, and concave utility function that satisfies (17).*
- 2) *There exist positive reals $u_t, \lambda_t > 0$, $t = 1, 2, \dots, N$, such that the following inequalities hold.*

$$u_s - u_t - \lambda_t \alpha'_t (\beta_s - \beta_t) \leq 0 \quad \forall t, s \in \{1, 2, \dots, N\}. \quad (18)$$

The monotone, concave utility function⁹ given by

$$U(\beta) = \min_{t \in \{1, 2, \dots, N\}} \{u_t + \lambda_t \alpha'_t (\beta - \beta_t)\} \quad (19)$$

constructed using u_t and λ_t defined in (18) rationalizes the dataset by satisfying (17).

- 3) *The data set \mathcal{D} satisfies the Generalized Axiom of Revealed Preference (GARP) also called cyclic consistency, namely for any $t \leq N$, $\alpha'_t \beta_t \geq \alpha'_t \beta_{t+1} \quad \forall t \leq k-1 \implies \alpha'_k \beta_k \leq \alpha'_k \beta_1$.*

Afriat’s theorem tests for economics-based rationality; its remarkable property is that it gives a *necessary and sufficient condition* for a system to be a utility maximizer based on the system’s input-output response. Although GARP in statement 4 in Theorem III.2 is not critical to the developments in this paper, it is of high significance in micro-economic theory and is stated here for completeness. The feasibility of the set of inequalities (18) can be checked using a linear programming solver; alternatively GARP can be checked using Warshall’s algorithm with $O(N^3)$ computations [39], [37].

The recovered utility using (19) is not unique; indeed any positive monotone increasing transformation of (19) also satisfies Afriat’s Theorem; that is, the utility function constructed is

⁹As pointed out in [37], a remarkable feature of Afriat’s theorem is that if the dataset can be rationalized by a monotone utility function, then it can be rationalized by a continuous, concave, monotonic utility function. Put another way, continuity and concavity cannot be refuted with a finite dataset.

ordinal. This is the reason why the budget constraint $\alpha'_n \beta \leq 1$ is without generality; it can be scaled by an arbitrary positive constant and Theorem III.2 still holds. In signal processing terminology, Afriat’s Theorem can be viewed as set-valued system identification of an *argmax* system; set-valued since (19) yields a set of utility functions that rationalize the finite dataset \mathcal{D} .

B. Beam Allocation: Revealed Preference Test

This section constructs a test to identify a cognitive radar that switches its beam adaptively between targets. This example is based on [25] and is presented here for completeness. The setup is schematically shown in Figure 4. We view each component i of the probe signal $\alpha_n(i)$ as the trace of the information matrix (inverse covariance) of target i . We use the trace of the information matrix of each target in our probe signal – this allows us to consider multiple targets. Since the adversarial radar is assumed to be stationary, the target covariance used to define the probe for the radar is indeed the maneuver covariance.

The setup in Figure 4 differs significantly from the setup of Figure 2 considered in the previous section. First, the adversary in the current setup is an economically rational agent. In Figure 2, the adversary is only specified at a lower level of abstraction as using a Bayesian filter to track our maneuvers. Second, this section abstracts adversary’s actions at the fast time scale indexed by k by an appropriately defined response at the slow time scale indexed by n . The previous section’s analysis was confined to the actions generated only at the fast time scale k . Lastly, Figure 4 assumes the abstracted response β_k of the adversary is measured accurately by us as opposed to a noisy measurement a_k of the adversary’s action u_k in Figure 2.

Suppose a radar adaptively switches its beam between m targets where these m targets are controlled by us. As in (4), on the fast time scale indexed by k , each target i has linear Gaussian dynamics and the adversary radar obtains linear Gaussian measurements:

$$\begin{aligned} x_{k+1}^i &= A x_k^i + w_k^i, & x_0 &\sim \pi_0 \\ y_k^i &= C x_k^i + v_k^i, & i &= 1, 2, \dots, m \end{aligned} \quad (20)$$

Here $w_k^i \sim \mathbf{N}(0, Q_n(i))$, $v_k^i \sim \mathbf{N}(0, R_n(i))$. Recall from Figure 4 that n indexes the epoch (slow time scale) and k

indexes the fast time scale within the epoch. We assume that both $Q_n(i)$ and $R_n(i)$ are known to us and the adversary.

The adversary's radar tracks our m targets using Kalman filter trackers. The fraction of time the radar allocates to each target i in epoch n is $\beta_n(i)$. The price the radar pays for each target i at the beginning of epoch n is the trace of the predicted *accuracy* of target i . Recall that this is the trace of the inverse of the predicted covariance at epoch n using the Kalman predictor

$$\alpha_n(i) = \text{Tr}(\Sigma_{n|n-1}^{-1}(i)), \quad i = 1, \dots, m \quad (21)$$

The predicted covariance $\Sigma_{n|n-1}(i)$ is a deterministic function of the maneuver covariance $Q_n(i)$ of target i . So the probe¹⁰ $\alpha_n(i)$ is a signal that we can choose, since it is a deterministic function of the maneuver covariance $Q_n(i)$ of target i . We abstract the target's covariance by its trace denoted by $\alpha_n(i)$. Note also that the observation noise covariance $R_n(i)$ depends on the adversary's radar response $\beta_n(i)$, i.e., the fraction of time allocated to target i . We assume that each target i can estimate the fraction of time $\beta_n(i)$ the adversary's radar allocates to it using a radar detector.

Given the time series $\alpha_n, \beta_n, n = 1, \dots, N$, our aim is to detect if the adversary's radar is cognitive. We assume that a cognitive radar optimizes its beam allocation as the following constrained optimization:

$$\begin{aligned} \beta_n &= \underset{\beta}{\text{argmax}} U(\beta) \\ \text{s.t. } \beta^t \alpha_n &\leq p_*, \end{aligned} \quad (22)$$

where $U(\cdot)$ is the adversary radar's utility function (unknown to us) and $p_* \in \mathbb{R}_+$ is a pre-specified average accuracy of all m targets.

The economics-based rationale for the budget constraint is natural: For targets that are cheaper (lower accuracy $\alpha_n(i)$), the radar has incentive to devote more time $\beta_n(i)$. However, given its resource constraints, the radar can achieve at most an average accuracy of p_* over all targets.

The setup in (22) is directly amenable to Afriat's Theorem III.2. Thus (18) can be used to test if the radar satisfies utility maximization in its beam scheduling (22) and also estimate the set of utility functions (19). Furthermore (as in Afriat's theorem) since the utility is ordinal, p_* can be chosen as 1 without loss of generality (and therefore does not need to be known by us).

C. Waveform adaptation: Revealed Preference Test for Non-linear budgets

In the previous subsection, we tested for cognitiveness of a radar by viewing it as an abstract system that switches its beam adaptively between targets. Here, we discuss cognitiveness with respect to waveform design. Specifically, we construct a test to identify cognitive behavior of an adversary radar that

¹⁰In comparison to (4), the velocity and acceleration elements of x_k^i in (20) must be multiplied by normalization factors Δt and $(\Delta t)^2$ respectively, for (21) to be dimensionally correct, where Δt is the time duration between two discrete time instants on the fast time scale.

optimizes its waveform based on the SINR of the target measurement. By using a generalization of Afriat's theorem (Theorem III.2) to non-linear budgets, our main aim is to detect if a radar intelligently chooses its waveform to maximize an underlying utility subject to signal processing constraints. Our setup below differs from [25] since we introduce the SINR as a nonlinear budget constraint; in comparison [25] uses a spectral budget constraint.

We start by briefly outlining the generalized utility maximization setup.

Definition III.3 ([16]). *A system is a generalized utility maximizer if for every probe $\alpha_n \in \mathbb{R}_+^m$, the response $\beta_n \in \mathbb{R}^m$ satisfies*

$$\beta_n \in \underset{g_n(\beta) \leq 0}{\text{argmax}} U(\beta) \quad (23)$$

where $U(\beta)$ is a monotone utility function and $g_n(\cdot)$ is monotonically increasing in β .

The above utility maximization model generalizes Definition III.1 since the budget constraint $g_n(\beta) \leq 0$ can accommodate non-linear budgets and includes the linear budget constraint of Definition III.1 as a special case. The result below provides an explicit test for a system that maximizes utility in the sense of Definition III.3 and constructs a set of utility functions that rationalizes the decisions β_n of the utility maximizer.

Theorem III.4 (Test for rationality with nonlinear budget [16]). *Let $B_n = \{\beta \in \mathbb{R}_+^m | g_n(\beta) \leq 0\}$ with $g_n : \mathbb{R}^m \rightarrow \mathbb{R}$ an increasing, continuous function and $g_n(\beta_n) = 0$ for $n = 1, \dots, N$. Then the following conditions are equivalent:*

- 1) *There exists a monotone continuous utility function U that rationalizes the data set $\{\beta_n, B_n\}, n = 1, \dots, N$. That is*

$$\beta_n = \underset{\beta}{\text{argmax}} U(\beta), \quad g_n(\beta) \leq 0$$

- 2) *There exist positive reals $u_t, \lambda_t > 0, t = 1, 2, \dots, N$, such that the following inequalities hold.*

$$u_s - u_t - \lambda_t g_t(\beta_s) \leq 0 \quad \forall t, s \in \{1, 2, \dots, N\} \quad (24)$$

The monotone, concave utility function given by

$$U(\beta) = \min_{t \in \{1, \dots, N\}} \{u_t + \lambda_t g_t(\beta)\} \quad (25)$$

constructed using u_t and λ_t defined in (24) rationalizes the data set by satisfying (23).

- 3) *The data set $\{\beta_n, B_n\}, n = 1, \dots, N$ satisfies GARP:*

$$g_t(\beta_j) \leq g_t(\beta_t) \implies g_j(\beta_t) \geq 0 \quad (26)$$

Like Afriat's theorem, the above result provides a *necessary and sufficient condition* for a system to be a utility maximizer based on the system's input-output response. In spite of a non-linear budget constraint, it can be easily verified that the constructed utility function $U(\beta)$ (25) is ordinal since any positive monotone increasing transformation of (25) satisfies the GARP inequalities (26).

We now justify the non-linear budget constraint in (23) in the context of the cognitive radar by formulating an optimization problem the radar solves equivalent to Definition III.3.

Suppose we observe the radar over $n = 1, 2, \dots, N$ time epochs (slow varying time scale). At the n^{th} epoch, we probe the radar with an interference vector $\alpha_n \in \mathbb{R}^M$. The radar responds with waveform $\beta_n \in \mathbb{R}_+^M$. We assume the chosen waveform β_n maximizes the radar's underlying utility function while ensuring the radar's SINR exceeds a particular threshold $\delta > 0$, where the SINR of the radar given probe α and response β is defined as

$$\text{SINR}(\alpha, \beta) = \frac{\beta' Q \beta}{\beta' P(\alpha) \beta + \gamma}. \quad (27)$$

In (27), the radar's signal power (numerator) and interference power (first term in denominator) are assumed to be quadratic forms of $Q, P(\alpha)$ respectively, where $Q, P(\alpha) \in \mathbb{R}^{M \times M}$ are positive definite matrices known to us. The term $\gamma > 0$ is the noise power. The SINR definition in (27) is a more general formulation of the SCNR (33) of a cognitive radar derived in Sec. IV using clutter response models [17]. The matrices $Q, P(\alpha)$ are analogous to the covariance of the channel impulse response matrices $H_t(\cdot)$ and $H_p(\cdot)$ corresponding to the target and clutter (external interference) channels, respectively (see Sec. IV-A for a discussion).

Having defined the SINR above in (27), we now formalize the radar's response β_n given probe α_n , $n = 1, 2, \dots$ as the solution of the following constrained optimization problem.

$$\begin{aligned} \beta_n &\in \underset{\beta}{\text{argmax}} U(\beta) \\ \text{s.t. } \text{SINR}(\alpha_n, \beta) &\geq \delta \end{aligned} \quad (28)$$

Clearly, the above setup falls under the non-linear utility maximization setup in Definition III.3 by defining the non-linear budget $g_n(\cdot)$ as $g_n(\beta) = \delta - \text{SINR}(\alpha_n, \beta)$ where $\text{SINR}(\cdot)$ is defined in (27). It only remains to show that this definition of $g_n(\beta)$ is monotonically increasing in β . Theorem III.5 stated below establishes two conditions that are sufficient for $g_n(\beta)$ to be monotonically increasing in β .

Theorem III.5. *Suppose that the adversary radar uses the SINR constraint (28). Then $g_n(\beta) = \delta - \text{SINR}(\alpha_n, \beta)$ is monotonically increasing in β if the following two conditions hold.*

- 1) *The matrix Q is a diagonal matrix with off-diagonal elements equal to zero.*
- 2) *The matrix $\left(\frac{c_{P(\alpha_n)}}{d_Q} P(\alpha_n) - Q\right)$ is component-wise less than 0 for all $n \in \{1, 2, \dots, N\}$, where $c_{P(\alpha_n)} > 0$ and $d_Q > 0$ denote the smallest and largest eigenvalues of $P(\alpha_n)$ and Q respectively.*

The proof of Theorem III.5 follows from elementary calculus and omitted for brevity. Hence, assuming the two conditions hold in Theorem III.5 above, we can use the results from Theorem III.4 to test if the radar satisfies utility maximization in its waveform design (28) and also estimate the set of feasible utility functions $U(\cdot)$ (28) that rationalizes the radar's responses $\{\beta_n\}$.

IV. DESIGNING SMART INTERFERENCE TO CONFUSE COGNITIVE RADAR

This section discusses how we can engineer (design) external interference (a probing signal) at the physical layer level to confuse a cognitive radar. By abstracting the probing signal to a channel in the frequency domain, our objective is to minimize the signal power of the interference generated by us while ensuring the SCNR of the radar does not exceed a pre-defined threshold. The setup is schematically shown in Figure 5. Note that the level of abstraction used in this section is at the Wiener filter pulse/waveform level; whereas the previous two sections were at the systems level (which uses the utility maximization framework) and tracker level (which uses the Kalman filter formalism), respectively. This is consistent with the design theme of sense globally (high level of abstraction) and act locally (lower level of abstraction).

As can be seen in the SCNR expression (33), the interference signal power manifests as additional clutter perceived by the radar in the denominator thus forcing the SCNR to go down. The radar then re-designs its waveform to maximize its SCNR given our interference signal. We observe the adversarial radar's chosen waveform in noise. Our task can thus be re-formulated as choosing the interference signal with minimal power while ensuring that with probability at least $1 - \epsilon$, the optimized SCNR lies below a threshold level Δ . Here, ϵ and Δ are user-defined parameters. This approach closely follows the formulation in Sec. III-C where the cognitive radar chooses the optimal waveform while ensuring the SINR exceeds a threshold value. Further, the SCNR of the adversary's radar defined in (34) below can be interpreted as a monotone function of the radar's utility function in the abstracted setup of Sec. III-C, since in complete analogy to the utility maximization model of Sec. III-C, this section assumes the radar maximizes its SCNR in the presence of smart interference signals (probes).

A. Interference Signal Model

We first characterize how a cognitive radar optimally chooses its waveform based on its perceived interference. The radar's objective is to choose the optimal waveform that maximizes its signal-to-interference-plus-noise (SINR) ratio.

Suppose we observe the adversarial radar over $l = 1, 2, \dots, L$ pulses, where each pulse comprises $n = 1, 2, \dots, N$ discrete time steps. A single-input single-output (SISO) radar system has two channel impulse responses, one for the target and the other for clutter. Let $w(n)$ denote the radar transmit waveform and $h_t(n)$, $h_c(n)$ denote the target and clutter channel impulse responses, respectively. Then, the radar measurements corresponding to the l -th pulse can be expressed as

$$x(n, l) = h_t(n, l) \otimes w(n, l) + h_c(n, l) \otimes w(n, l) + e_r(n, l) \quad (29)$$

where \otimes represents a convolution operator and $e_r(n, l)$ is the radar measurement noise modeled as an i.i.d random variable with zero mean and known variance σ_r^2 . We model the radar's measurement using the stochastic Green's function impulse response model presented in [17], where the radar's

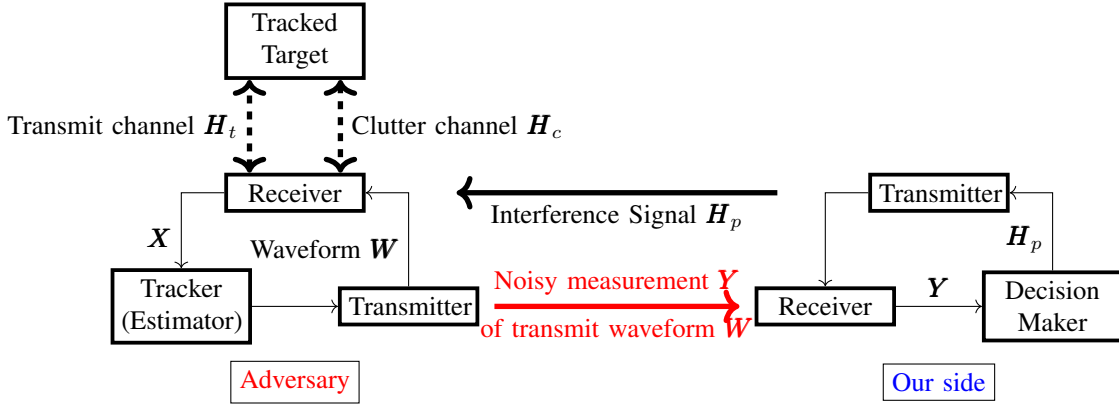


Fig. 5: Schematic of transmit channel H_t , clutter channel H_c and interference signal H_p involving an adversarial cognitive radar and us. We observe the radar's waveform W in noise. The aim is to engineer the interference signal H_p to confuse the adversary cognitive radar.

electromagnetic channel is modeled using a physics based impulse response.

Since convolution in the time domain can be expressed as multiplication in the frequency domain (with notation in upper case), we can express the measurements in the frequency domain as follows:

$$X(k, l) = H_t(k, l)W(k, l) + H_c(k, l)W(k, l) + E_r(k, l) \quad (30)$$

where $k \in \mathcal{K} = \{1, \dots, K\}$ is the frequency bin index. Eq. (30) can be extended to an $I \times J$ MIMO radar and the received signal at the j -th receiver is given by

$$X_j(k, l) = \sum_{i=1}^I H_{t_{ij}}(k, l)W_i(k, l) + H_{c_{ij}}(k, l)W_i(k, l) + E_{r,j}(k, l), \quad (31)$$

$\forall k \in \{1, \dots, K\}$. Using matrices and vectors obtained by stacking and concatenating (31) for all i, j , and k , the MIMO radar measurement model at the l^{th} pulse in vector-matrix form can be expressed as

$$\mathbf{X}(l) = \mathbf{H}_t(l)\mathbf{W}(l) + \mathbf{H}_c(l)\mathbf{W}(l) + \mathbf{E}_r(l) \quad (32)$$

where $\mathbf{X}(l) \in \mathbb{C}^{(J \times K) \times 1}$ is the received signal vector, $\mathbf{H}_c(l), \mathbf{H}_t(l) \in \mathbb{C}^{(J \times K) \times (I \times J \times K)}$ are the effective transmit and clutter channel impulse response matrices respectively, $\mathbf{W}(l) \in \mathbb{C}^{(I \times J \times K) \times 1}$ is the radar's effective waveform vector. $\mathbf{E}_r(l) \in \mathbb{C}^{(J \times K) \times 1}$ is the effective additive noise vector modeled as a zero mean i.i.d random variable (independent over pulses) with covariance matrix $C_r \in \mathbb{R}^{(J \times K) \times (J \times K)}$, $C = (\sigma_r^2/K)\mathbf{I} = \tilde{\sigma}_r^2\mathbf{I}$. The block diagram in Fig. 5 shows the entire procedure for this model.

B. Smart Interference to confuse the adversary radar

The aim of this section is to design optimal interference signals (to confuse the adversary cognitive radar) by solving a probabilistically constrained optimization problem.

At the beginning of the l^{th} pulse, the adversary radar transmits a pilot signal to estimate the transmit and clutter channel impulse responses $\mathbf{H}_t(l)$ and $\mathbf{H}_c(l)$ respectively. Assuming it has a perfect estimate of $\mathbf{H}_t(l)$ and $\mathbf{H}_c(l)$, the radar then

chooses the optimal waveform $\mathbf{W}^*(l)$ such that SCNR defined below in (33) is maximized. The radar's waveform $\mathbf{W}^*(l)$ is the solution to the following optimization problem

$$\mathbf{W}^*(l) = \underset{\mathbf{W}(l): \|\mathbf{W}(l)\|_2=1}{\operatorname{argmax}} \operatorname{SCNR}(\mathbf{H}_t(l), \mathbf{H}_c(l), \mathbf{W}(l)), \quad (33)$$

where the SCNR is defined as

$$\operatorname{SCNR}(\mathbf{H}_t, \mathbf{H}_c, \mathbf{W}) = \frac{\|\mathbf{H}_t\mathbf{W}\|_2^2}{\mathbb{E}\left\{\|\mathbf{H}_c\mathbf{W} + \mathbf{E}_r\|_2^2\right\}}. \quad (34)$$

Denote the maximum SCNR achieved in (33) as

$$\operatorname{SCNR}_{\max}(\mathbf{H}_t(l), \mathbf{H}_c(l), \sigma_r^2) = \operatorname{SCNR}(\mathbf{H}_t(l), \mathbf{H}_c(l), \mathbf{W}^*(l)). \quad (35)$$

Given $\mathbf{H}_t(l), \mathbf{H}_c(l)$ and the radar's measurement noise power σ_r^2 , the radar generates an optimal waveform at the l^{th} pulse using (33) as the solution to the following eigenvector problem [5]:

$$\begin{aligned} \mathbf{A}\mathbf{W}^*(l) &= \lambda_l\mathbf{W}^*(l) \\ \mathbf{A} &= \left((\mathbf{H}_c(l)'\mathbf{H}_c(l) + \tilde{\sigma}_r^2\mathbf{I})^{-1}\mathbf{H}_t(l)'\mathbf{H}_t(l) \right), \end{aligned}$$

Here $(\cdot)'$ denotes the Hermitian transpose operator.

As an external observer, we send a sequence of probe signals $P = \{\mathbf{H}_p(l), l \in \{1, 2, \dots, L\}\}$ over L pulses to confuse the adversary radar and degrade its performance. The interference signal $\mathbf{H}_p(l-1)$ at the $(l-1)^{th}$ affects only radar's clutter channel impulse response $\mathbf{H}_c(l)$ at the l^{th} pulse which subsequently results in change of optimal waveform (33) chosen by the radar $\mathbf{W}^*(l)$. We measure the optimal waveform at the l^{th} pulse in noise as $\mathbf{Y}(l)$. We assume constant transmit and clutter channel impulse responses $\mathbf{H}_t, \mathbf{H}_c$ in the absence of the probe signals P . The dynamics of our interaction with the adversary radar due to probe P are as follows and

schematically shown in Fig. 6:

$$\mathbf{H}_c(l) = \mathbf{H}_c + \mathbf{H}_p(l-1) \quad (36)$$

$$\mathbf{H}_t(l) = \mathbf{H}_t \quad (37)$$

$$\begin{aligned} & \left((\mathbf{H}_c(l)' \mathbf{H}_c(l) + \tilde{\sigma}_r^2 \mathbf{I})^{-1} \mathbf{H}_t(l)' \mathbf{H}_t(l) \right) \mathbf{W}^*(l) \\ & = \lambda_l \mathbf{W}^*(l) \end{aligned} \quad (38)$$

$$\mathbf{Y}(l) = \mathbf{W}^*(l) + \mathbf{E}_o(l). \quad (39)$$

In (39), $\mathbf{E}_o(l)$ is our measurement noise modeled as a zero mean i.i.d random variable (independent over pulses) sampled from a known pdf f_o with zero mean and covariance $\mathbf{C}_o = (\sigma_o^2/K) \mathbf{I} = \tilde{\sigma}_o^2 \mathbf{I}$.

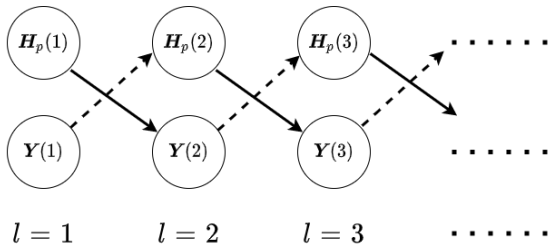


Fig. 6: Schematic of smart interference design to confuse the cognitive radar. The interference signal at the l^{th} pulse affects the waveform choice of the radar in the $(l+1)^{\text{th}}$ pulse. We record the noisy waveform measurement $\mathbf{Y}(l+1)$ and generate the interference signal for the $(l+2)^{\text{th}}$ pulse.

Our objective is to optimally design the probe signals $\mathbf{P}^* = \{\mathbf{H}_p^*(l), l \in \{1, \dots, L\}\}$ that minimizes the interference signal power such that for a pre-defined $\Delta > 0$, there exists $\epsilon \in [0, 1)$ such that the probability the SCNR of the radar lies below Δ exceeds $(1 - \epsilon)$, for all $l = 1, 2, \dots, L$.

$$\begin{aligned} & \min_{\{\mathbf{H}_p(l), l \in \{1, 2, \dots, L\}\}} \sum_{l=1}^L \mathbf{H}_p(l)' \mathbf{H}_p(l) \\ & \text{s.t. } \mathbb{P}_{f_o}(\text{SCNR}(\mathbf{H}_t(l), \mathbf{H}_c(l), \mathbf{Y}(l)) \leq \Delta) \geq 1 - \epsilon, \\ & \quad \forall l \in \{1, 2, 3, \dots, L\}. \end{aligned} \quad (40)$$

Here, $\mathbb{P}_f(\cdot)$ denotes the probability wrt pdf f . The design parameter Δ is the SCNR (performance) upper bound of the cognitive radar. To confuse the radar, our task is to ensure the SCNR of the radar is less than Δ with probability at least $1 - \epsilon$. Hence, ϵ is the maximum probability of failure to confuse the radar with our smart interference signals. Although not explicitly shown, the SCNR_{\max} expression in (40) depends on our interference signal \mathbf{H}_p as depicted in (36).

Solving the non-convex optimization problem (40) is challenging except for trivial cases. It involves two inter-related components (i) Estimating the transmit and clutter channel impulse responses $\mathbf{H}_t, \mathbf{H}_c$ from observation $\mathbf{Y}(l)$ and (ii) Using the estimated value of channel impulse responses to generate the interference signal $\mathbf{H}_p(l)$. Moreover, solving for \mathbf{H}_c and \mathbf{H}_t from recursive equations (36) through (39) for $l = 1, \dots, L$ is a challenging problem since it does not have an analytical closed form solution.

With the above formulation, we can now discuss construction of smart inference to confuse the adversary radar. The

cognitive radar maximizes its energy in the direction of its target impulse response and transfer function. As soon as we have an accurate estimate of the target channel transfer function from the L pulses, we can immediately generate signal dependent interference that nulls the target returns. Even if the clutter channel impulse response changes after we perform our estimation, since the target channel is stationary for longer durations, the signal dependent interference will work successfully for several pulses after we compute the estimate. The main take away from this approach is that we are exploiting the fact that the cognitive radar provides information about its channel by optimizing the waveform with respect to its environment.

C. Numerical example illustrating design of smart interference

We conclude this section with a numerical example that illustrates the smart interference framework developed above. The simulation setup is as follows:

- $L = 2$ pulses (optimization horizon in (40)).
- Impulse response matrices for transmit channel $\mathbf{H}_t = [7 \ 7]$, clutter channel $\mathbf{H}_c = [1 \ 1]$, and adversary radar noise covariance $\tilde{\sigma}_r^2 = 1$ (32).
- *Design parameters:* SCNR upper bound $\Delta = \{2.8, 3, 3.2\}$, minimum probability of success $\epsilon = 0.2, 0.3$ (40).
- Probe signals for pulse index:

$$\begin{aligned} l = 1, \quad \mathbf{H}_p(1) &= [0.2r \ 0.5r], \\ l = 2, \quad \mathbf{H}_p(2) &= [0.4r \ 0.4r]. \end{aligned} \quad (41)$$

The smart interference parameter $r > 0$ parametrizes the magnitude of the probe signals. The aim is to find the optimal probe signals $\mathbf{H}_p(l)$, $l = 1, 2$ parametrized by r in (41) that solves (40). The corresponding value of r is our optimal smart interference parameter.

- Our measurement noise covariance is $\tilde{\sigma}_o^2 = 0.1$ (39).
- Figure 7 displays the performance of the cognitive radar as our smart interference parameter r is varied. It shows that increasing r leads to increased confusion (worse SCNR performance) of the cognitive radar. Specifically, we plot the LHS of (40), namely, $\mathbb{P}_{f_o}(\text{SCNR}(\mathbf{H}_t(l), \mathbf{H}_c(l), \mathbf{Y}(l)) \leq \Delta)$, for SCNR upper bound $\Delta \in \{2.8, 3, 3.2\}$. Recall that this is the probability with which the maximum SCNR of the radar (35) lies below Δ .

To glean insight from Figure 7, let $r^*(\Delta, \epsilon)$ denote the optimal smart interference parameter that solves (40) for design parameters Δ and ϵ . Figure 7 shows that $r^*(\Delta, \epsilon)$ decreases with both design parameters Δ and ϵ . This can be justified as follows. For a fixed value of failure probability ϵ , increasing the upper bound Δ implies the constraint (40) is satisfied for smaller r , hence the optimal interference parameter $r^*(\Delta, \epsilon)$ decreases with Δ . Recall ϵ upper bounds the probability with which the maximum SCNR of the radar exceeds Δ . Increasing ϵ (or equivalently, relaxing the maximum probability of failure) allows us to decrease the magnitude of the probe signals without violating the constraint in (40) for a fixed Δ . Hence, $r^*(\Delta, \epsilon)$ decreases with both Δ and ϵ .

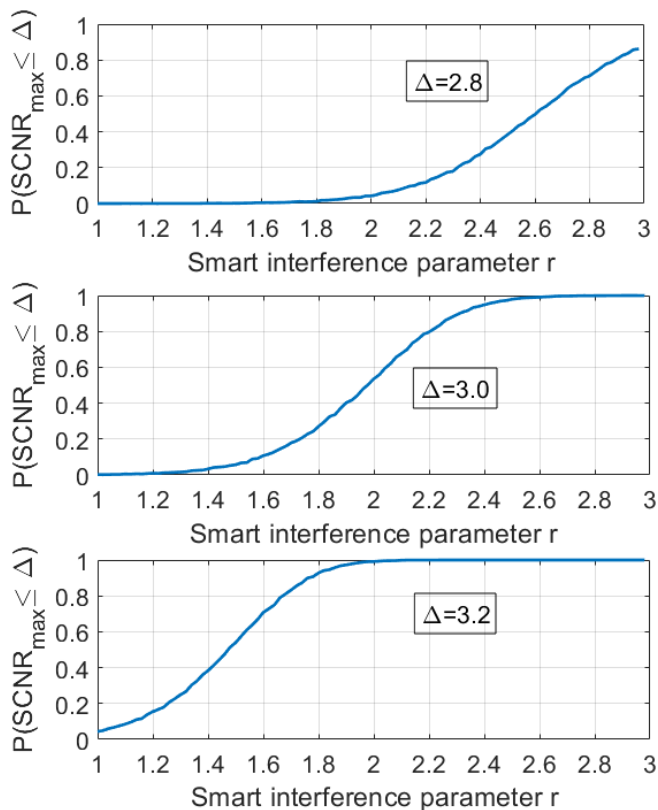


Fig. 7: The figure illustrates the performance of the cognitive radar as our smart interference parameter r in (41) is varied. The plots display the LHS of (40), namely, probability that the radar’s maximum SCNR (which depends on r (41)) is smaller than threshold Δ . The probability curves are plotted for $\Delta = 2.8, 3, 3.2$ and signify the extent of SCNR degradation as a function of the magnitude of the probe signal.

V. CONCLUSION

This paper considered three important inter-related aspects of adversarial inference involving cognitive radars. First we discussed inverse tracking (estimating the adversary tracker’s estimate based on the radar’s actions) and calibration of the adversary’s sensor accuracy. Then we presented a revealed preferences methodology for identifying cognitive radars; i.e., identifying a constrained utility maximizer. Finally, we discussed designing interference to confuse the cognitive radar. The above three aspects are inter-related as depicted in Figure 1. The levels of abstraction range from smart interference design based on Wiener filters (at the pulse/waveform level), inverse Kalman filters at the tracking level and revealed preferences for identifying utility maximization at the systems level.

Extensions: The results in this paper lead to several interesting future extensions. There is strong motivation to determine analytic performance bounds for inverse tracking/filtering and estimation of the adversary’s sensor gain. Another aspect (not considered here) is when the adversary does not know the transition kernel of our dynamics; the adversary then needs to estimate this transition kernel, and we need to estimate the estimate of this transition kernel. In future work we will design

the smart interference problem (40) as a stochastic control problem; since dynamic programming is intractable we will explore limited look-ahead policies and open-loop feedback control.

Regarding identifying cognitive radars, it is worthwhile developing statistical tests for utility maximization when the response of the utility maximizing adversarial radar is observed in noise; see Varian’s work [39] on noisy revealed preference. Ongoing research in developing a dynamic revealed preference framework will be used to extend the beam allocation problem of Sec. III-B to a multi-horizon setup where we analyze batches of adversary responses over multiple slow time scale epochs. Another natural extension is to a Bayesian context, namely, identifying a radar that is a Bayesian utility maximizer. We refer to [7] for seminal work in this area stemming from behavioral economics.

Finally, in the design of controlled inference, it is worthwhile considering a game-theoretic setting where the cognitive radar (adversary) and us interact dynamically. In previous work [32] we studied simpler versions of the problem in the context of cross-polarized jamming. Also, in future work, it is worthwhile to develop a stochastic gradient algorithm for estimating the optimal probe signal.

REFERENCES

- [1] S. Afriat. The construction of utility functions from expenditure data. *International economic review*, 8(1):67–77, 1967.
- [2] S. Afriat. *Logic of choice and economic theory*. Clarendon Press Oxford, 1987.
- [3] B. D. O. Anderson and J. B. Moore. *Optimal filtering*. Prentice Hall, Englewood Cliffs, New Jersey, 1979.
- [4] G. Angeletos, C. Hellwig, and A. Pavan. Dynamic global games of regime change: Learning, multiplicity, and the timing of attacks. *Econometrica*, 75(3):711–756, 2007.
- [5] J. S. Bergin, J. R., R. M. Guerri, and M. Rangaswamy. MIMO Clutter Discrete Probing for Cognitive Radar. In *IEEE International Radar Conference*, pages 1666–1670, April 2015.
- [6] P. Caines. *Linear Stochastic Systems*. Wiley, 1988.
- [7] A. Caplin and M. Dean. Revealed preference, rational inattention, and costly information acquisition. *The American Economic Review*, 105(7):2183–2203, 2015.
- [8] O. Cappe, E. Moulines, and T. Ryden. *Inference in Hidden Markov Models*. Springer-Verlag, 2005.
- [9] J. Cavanaugh and R. Shumway. On computing the expected fisher information matrix for state space model parameters. *Statistics & Probability Letters*, 26:347–355, 1996.
- [10] C. Chamley. *Rational herds: Economic Models of Social Learning*. Cambridge University Press, 2004.
- [11] E. K. P. Chong, C. Kreucher, and A. Hero. Partially observable Markov decision process approximations for adaptive sensing. *Discrete Event Dynamic Systems*, 19(3):377–422, 2009.
- [12] D. Ciunzo, P. K. Willett, and Y. Bar-Shalom. Tracking the tracker from its passive sonar ml-pda estimates. *IEEE Transactions on Aerospace and Electronic Systems*, 50(1):573–590, 2014.
- [13] P. Del Moral, E. Rio, et al. Concentration inequalities for mean field particle models. *Annals of Applied Probability*, 21(3):1017–1052, 2011.
- [14] W. Diewert. Afriat’s theorem and some extensions to choice under uncertainty. *The Economic Journal*, 122(560):305–331, 2012.
- [15] R. J. Elliott, L. Aggoun, and J. B. Moore. *Hidden Markov Models – Estimation and Control*. Springer-Verlag, New York, 1995.
- [16] F. Forges and E. Minelli. Afriat’s theorem for general budget sets. *Journal of Economic Theory*, 144(1):135–145, 2009.
- [17] J. Guerri, J. Bergin, R. Guerri, M. Khanin, and M. Rangaswamy. A new MIMO clutter model for cognitive radar. In *2016 IEEE Radar Conference (RadarConf)*, pages 1–6. IEEE, 2016.
- [18] J. R. Guerri, J. S. Bergin, R. J. Guerri, M. Khanin, and M. Rangaswamy. A New MIMO Clutter Model for Cognitive Radar. In *IEEE Radar Conference*, May 2016.

- [19] S. Haykin. Cognitive radar. *IEEE Signal Processing Magazine*, pages 30–40, Jan. 2006.
- [20] S. Haykin. Cognitive dynamic systems: Radar, control, and radio [point of view]. *Proceedings of the IEEE*, 100(7):2095–2103, 2012.
- [21] C.-C. Huang, B. Amini, and R. R. Bitmead. Predictive coding and control. *IEEE Transactions on Control of Network Systems*, 6(2):906–918, 2018.
- [22] V. Krishnamurthy. Bayesian sequential detection with phase-distributed change time and nonlinear penalty – a lattice programming POMDP approach. *IEEE Transactions on Information Theory*, 57(3):7096–7124, Oct. 2011.
- [23] V. Krishnamurthy. Quickest detection POMDPs with social learning: Interaction of local and global decision makers. *IEEE Transactions on Information Theory*, 58(8):5563–5587, 2012.
- [24] V. Krishnamurthy. *Partially Observed Markov Decision Processes. From Filtering to Controlled Sensing*. Cambridge University Press, 2016.
- [25] V. Krishnamurthy, D. Angley, R. Evans, and W. Moran. Identifying cognitive radars - inverse reinforcement learning using revealed preferences. *IEEE Transactions on Signal Processing*, 2019 (in press; also available on arxiv: <https://arxiv.org/abs/1912.00331>).
- [26] V. Krishnamurthy and D. Djonin. Structured threshold policies for dynamic sensor scheduling—a partially observed Markov decision process approach. *IEEE Transactions on Signal Processing*, 55(10):4938–4957, Oct. 2007.
- [27] V. Krishnamurthy and D. Djonin. Optimal threshold policies for multivariate POMDPs in radar resource management. *IEEE Transactions on Signal Processing*, 57(10), 2009.
- [28] V. Krishnamurthy, E. Leoff, and J. Sass. Filterbased stochastic volatility in continuous-time hidden Markov models. *Econometrics and statistics*, 6:1–21, 2018.
- [29] V. Krishnamurthy and M. Rangaswamy. How to calibrate your adversary’s capabilities? inverse filtering for counter-autonomous systems. *IEEE Transactions on Signal Processing*, 67(24):6511–6525, 2019.
- [30] A. Kuptel. Counter unmanned autonomous systems (cuaxs): Priorities. policy. future capabilities. 2017.
- [31] J. Marion. *Finite Sample Bounds and Path Selection for Sequential Monte Carlo*. PhD thesis, Duke University, 2018.
- [32] M. Maskery and V. Krishnamurthy. Network-enabled missile deflection: Games and correlation equilibrium. *IEEE Transactions on Aerospace and Electronic Systems*, 43(3):843–863, July 2007.
- [33] R. Mattila, I. Lourenço, C. R. Rojas, V. Krishnamurthy, and B. Wahlberg. Estimating private beliefs of Bayesian agents based on observed decisions. *IEEE Control Systems Letters*, 2019.
- [34] R. Mattila, C. Rojas, V. Krishnamurthy, and B. Wahlberg. Inverse filtering for hidden Markov models. In *Advances in Neural Information Processing Systems*, pages 4204–4213, 2017.
- [35] R. Mattila, C. Rojas, V. Krishnamurthy, and B. Wahlberg. Inverse filtering for linear Gaussian state-space models. In *Proceedings of IEEE Conference on Decision and Control*, 2018.
- [36] B. Ristic, S. Arulampalam, and N. Gordon. *Beyond the Kalman Filter: Particle Filters for Tracking Applications*. Artech, 2004.
- [37] H. Varian. The nonparametric approach to demand analysis. *Econometrica*, 50(1):945–973, 1982.
- [38] H. Varian. Non-parametric tests of consumer behaviour. *The Review of Economic Studies*, 50(1):99–110, 1983.
- [39] H. Varian. Revealed preference. *Samuelsonian economics and the twenty-first century*, pages 99–115, 2006.
- [40] H. Varian. Revealed preference and its applications. *The Economic Journal*, 122(560):332–338, 2012.



Vikram Krishnamurthy (F’05) received the Ph.D. degree from the Australian National University in 1992. He is a professor in the School of Electrical & Computer Engineering, Cornell University. From 2002-2016 he was a Professor and Canada Research Chair at the University of British Columbia, Canada. His research interests include statistical signal processing and stochastic control in social networks and adaptive sensing. He served as Distinguished Lecturer for the IEEE Signal Processing Society and Editor-in-Chief of the IEEE Journal on Selected Topics in Signal Processing. In 2013, he was awarded an Honorary Doctorate from KTH (Royal Institute of Technology), Sweden. He is author of two books *Partially Observed Markov Decision Processes* and *Dynamics of Engineered Artificial Membranes and Biosensors* published by Cambridge University Press in 2016 and 2018, respectively.

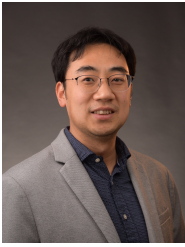


Kunal Pattanayak (S’21) received the integrated Bachelors and Masters in Technology degrees in Electronics and Electrical Communication Engineering from Indian Institute of Technology, Kharagpur in 2018. He is currently a graduate student in the department of Electrical and Computer Engineering at Cornell University. His research interests include inverse reinforcement learning, behavioral economics, statistical signal processing, design of counter-autonomous systems for radar applications and interpretable AI. He is a recipient of the Mc-Mullen graduate fellowship by Cornell University, and has been a speaker at the 2020 Sloan-NOMIS Conference on Attention and Applied Economics.



Sandeep Gogineni (BTech, Electronics and Communications Engineering, IIIT, India, MS, PhD, Electrical Engineering, Washington University in St. Louis) is a Research Scientist for Information Systems Laboratories with over 12 years of experience working on radar and wireless communications systems. He has worked for 6 years as an on-site contractor for Air Force Research Laboratory (AFRL), developing novel signal processing algorithms and performance analysis for passive radar systems. He received the IEEE Dayton Section Aerospace and

Electronics Systems Society Award for these contributions to passive radar signal processing. Prior to his time at AFRL, during his graduate studies at Washington University in St. Louis, Dr. Gogineni developed optimal waveform design techniques for adaptive MIMO radar systems and demonstrated improved target detection and estimation performance. At ISL, Dr. Gogineni has been working on channel estimation algorithms and optimal probing strategies for MIMO radar systems in the context of Cognitive Fully Adaptive Radar (CoFAR). Additionally, Dr. Gogineni and his colleagues at ISL have demonstrated the feasibility of using neural networks and artificial intelligence techniques to solve extremely challenging radio frequency (RF) sensing problems. His expertise includes statistical signal processing, detection and estimation theory, deep learning, artificial intelligence, performance analysis, and optimization techniques with applications to active and passive RF sensing systems.



Bosung Kang (S'12-M'16) received the B.S. and M.S. degrees in Electrical and Electronic Engineering from Yonsei University, Seoul, South Korea, in 2005 and 2007, respectively, and the Ph.D. degree in Electrical Engineering from the Pennsylvania State University, University Park, PA, USA, in 2015. He is currently an onsite contractor for Air Force Research Laboratory, WPAFB, OH and a radar research engineer at University of Dayton Research Institute, Dayton, OH. He worked at LG Electronics as a research engineer, Seoul, Korea, from 2007 to 2011.

He developed image and video signal processing algorithms in mobile camera and monitor applications. He has served as a reviewer for several reputed IEEE journals and conferences. His research interests include statistical signal processing, detection and estimation, convex optimization, and radar signal processing with applications to radar and communication systems. Dr. Kang was a recipient of the First Place in the Student Paper Competition at the IEEE Radar Conference, Cincinnati, OH, in 2014. He also won the 2015 Robert T. Hill Best Dissertation Award presented by the IEEE Aerospace and Electronic Systems Society (AESS).



Muralidhar Rangaswamy (Fellow, IEEE) received the B.E. degree in electronics engineering from Bangalore University, Bangalore, India, in 1985, and the M.S. and Ph.D. degrees in electrical engineering from Syracuse University, Syracuse, NY, USA, concurrently in 1992. He is currently the Technical Lead for Radar Sensing with the RF Technology Branch within the Sensors Directorate, Air Force Research Laboratory (AFRL), Wright-Patterson Air Force Base, OH, USA. Prior to this, he has held industrial and academic appointments. He is a contributor to eight books and is a co-inventor on three U.S. patents. He has coauthored more than 280 refereed journal and conference record papers in the areas of his research interests, which include radar signal processing, spectrum estimation, modeling non-Gaussian interference phenomena, and statistical communication theory. Dr. Rangaswamy is a member of the Radar Systems Panel (RSP) in the IEEE-AES Society. He was on the Technical Committee of the IEEE Radar Conference series in a myriad of roles. He was the recipient of the IEEE Warren White Radar Award in 2013, the 2013 Affiliate Societies Council Dayton (ASC-D) Outstanding Scientist and Engineer Award, the 2007 IEEE Region 1 Award, the 2006 IEEE Boston Section Distinguished Member Award, and the 2005 IEEE-AESS Fred Nathanson Memorial Outstanding Young Radar Engineer Award. He was also the recipient of the 2012 and 2005 Charles Ryan Basic Research Award from the Sensors Directorate, AFRL, in addition to more than 40 scientific achievement awards. Most recently, he received the International Society for Information Fusion Jean-Pierre Le Cadre Best Paper Award at the 2019 FUSION Conference, the 2019 Technical Cooperation Panel Award from the Office of Secretary of Defense, and the 2019 IEEE Dayton Section Fritz Russ Memorial Award.

He is a contributor to eight books and is a co-inventor on three U.S. patents. He has coauthored more than 280 refereed journal and conference record papers in the areas of his research interests, which include radar signal processing, spectrum estimation, modeling non-Gaussian interference phenomena, and statistical communication theory. Dr. Rangaswamy is a member of the Radar Systems Panel (RSP) in the IEEE-AES Society. He was on the Technical Committee of the IEEE Radar Conference series in a myriad of roles. He was the recipient of the IEEE Warren White Radar Award in 2013, the 2013 Affiliate Societies Council Dayton (ASC-D) Outstanding Scientist and Engineer Award, the 2007 IEEE Region 1 Award, the 2006 IEEE Boston Section Distinguished Member Award, and the 2005 IEEE-AESS Fred Nathanson Memorial Outstanding Young Radar Engineer Award. He was also the recipient of the 2012 and 2005 Charles Ryan Basic Research Award from the Sensors Directorate, AFRL, in addition to more than 40 scientific achievement awards. Most recently, he received the International Society for Information Fusion Jean-Pierre Le Cadre Best Paper Award at the 2019 FUSION Conference, the 2019 Technical Cooperation Panel Award from the Office of Secretary of Defense, and the 2019 IEEE Dayton Section Fritz Russ Memorial Award.